ROMANIAN JOURNAL OF INFORMATION SCIENCE AND TECHNOLOGY
Volume **18**, Number 4, 2015, 312–328

Dielectric Properties of LDH-Type Layered Materials Containing Zn or Mg Ions: On the Non Monotonous Temperature Dependence of Relaxation Times

Ligia FRUNZA[1], Stefan FRUNZA[1], Constantin Paul GANEA[1], Irina ZGURA[1], Florentina NEATU[2], Vasile I. PARVULESCU[2]

[1]National Institute of Materials Physics, R-077125 Magurele, Romania
[2]Dept. Chemical Technology and Catalysis, Faculty of Chemistry, University of Bucharest, R-030016 Bucharest, Romania

Corresponding author: lfrunza@infim.ro

Abstract. The electrical behavior of layered double hydroxides containing Al or Ga as the trivalent ions and Mg or Zn as bivalent ions was evaluated using broadband dielectric spectroscopy in a wide temperature range. Besides conduction effects a relaxation peak is observable at high frequencies which is assigned to the reorientational fluctuations of water molecules adsorbed on the oxide surface or in the interlayer voids. The Maxwell–Wagner–Sillars peak, superimposed to the conductivity phenomenon is observable at low frequencies. A non-monotonous temperature dependence of the relaxation rates of the relaxation process has been found. A quantitative description of this dependence was possible based on a model assuming two competing processes: rotational fluctuation of water molecules and formation of additional defects. Reasonable values for the characteristic parameters were obtained. Thus the water behavior in the studied layered oxides is similar to that observed for water in other porous materials. However, the activation energy of the rotational fluctuation, the pre exponential factor and the number of defects are higher whereas the value of the energy of defect formation is lower in the layered oxide materials than for water confined to nanoporous molecular sieves, porous glasses or in bulk ice.

1. Introduction

Layered double hydroxides (LDHs) or hydrotalcite-like materials are anionic clay materials [1]: a few anionic clays have been found in nature, but most of them can be readily synthesized in laboratory. These clay materials have attracted much attention because in the original or derived form they can have potential applications, especially as highly efficient catalysts in pharmaceutical industries and organic synthesis, as anion scavengers in wastewater treatments, medicine and health [2, 3]. They can be also used as photocatalysts [4]–[6]] for different reactions. LDHs have the property to be exfoliated into nanosheets [7] that can be further used as macromolecular building blocks in the assembly of nanocomposites, for the preparation of multifunctional materials with increasing levels of complexity. Thus, properties of pure polymers were improved by obtaining the polymer-based nanocomposites [8]–[10]. LDH materials are the basis for electrochemical biosensors [11], super-capacitors [12], vertically stacked artificial 2D materials [13], drug nanovehicles [14], remediation agents for environmental contaminants [15], multifunctional intercalation nanohybrids [16], supports for dye-sensitized solar cells [17] etc.

The structural and morphological properties of these materials were characterized by combination of several complementary methods as Rietveld analysis of powder X-ray diffraction diagrams, Differential Scanning Calorimetry (DSC), Small- and Wide-Angle X-ray Scattering (SAXS, WAXS), Scanning Electron Microscopy, Fourier Transform Infrared spectroscopy, Thermogravimetry etc. However, experimental studies probing the interlayer composition and properties, the surface regions and even the detailed structure of the sheets are revealed with difficulty and therefore are still scarcely discussed. To use the LDH based materials in a certain molecular electronic device, it is necessary to know their dynamic properties such as capacitance, conductivity, time relaxation and activation energy. That is why (broadband) dielectric spectroscopy measurements were already applied to layered materials or to their nanocomposites (to cite part of the recent works [18]–[28]).

Here we report more on the dielectric measurements in a few layered oxide materials positively charged, with the structure of LDHs containing bivalent (Mg^{2+} or Zn^{2+}) and trivalent (Al^{3+} or Ga^{3+}) ions in the framework and also anions (for electroneutrality) and water molecules in the interlayer space. An additional reason to complete thus the investigations in such materials is related to their application in catalytic reactions [29, 30]: the dynamics of the solvent/reactants or products is influenced by the catalyst structure. Based onto the dielectric behavior of the LDH nanocomposite materials [9], [19]–[23],[25]–[27] containing the same ion pairs as our samples but in different ratios, of the layered silicates [31]–[36] and of other layered (hydr)oxides [37]–[39], we expected changes in the dielectric properties with the composition of our samples due to the subtle balance of different forces including Coulomb repulsion, sterical hindrance, hydrophobic/hydrophilic interactions. Significant differences between the considered samples, which were related to their structure, were found.

2. Experimental Section

2.1. LDH materials

The structure of LDHs is similar to that of brucite ($Mg(OH)_2$) where each Mg^{2+} ion is octahedrally surrounded by hydroxyl groups. Isomorphous substitution of Mg^{2+} by a trivalent or other divalent ion can occur in the LDHs. When Mg^{2+} ions are replaced by a trivalent ion, a positive charge [1] is generated in the brucite sheet, which is otherwise electro neutral. The positive charge is compensated by the presence of anions in the interlayer. In these inter galleries there are also water molecules, leading to the following formula $[M^{2+}_{1-x}M^{3+}_x(OH)_2]^{x+}(A^{z-})_{x/z}\cdot mH_2O$. In our samples M^{2+}=Zn^{2+}, Mg^{2+}; M^{3+}=Al^{3+}, Ga^{3+}, $A^{z-}$are nitrate NO_3^- and/or carbonate CO_3^{2-}; the molar ratio M^{2+}/M^{3+} is 3 or 2. These samples were prepared by applying known recipes (as mentioned in refs. [29, 30, 40]) and were further noted Mg3Al-LDH, Mg3Ga-LDH, Zn2Al-LDH and Zn2Ga-LDH respectively. The obtained solids were finally dried at room temperature.

All the samples were routinely characterized by powder X-ray diffraction, FTIR (KBr technique) and nitrogen absorption.

2.2. Dielectric measurements

Self-supported pellets were pressed for the dielectric investigations just before the measurements and then handled in desiccators (see *e.g.* [39]). To remove some impurities the pellets were cleaned by vacuum (10^{-2} Torr) at room temperature for 2 h and then contacted for more than 24 h with water vapor under a controlled atmosphere. The water content of the samples was determined by thermogravimetric (TG) analysis (see below). The pellets were placed in a capacitor arrangement with parallel plate geometry. The measurements were conducted in a nitrogen stream, ensuring not only thermal equilibration but also protection of the sample from the surrounding atmosphere.

The complex dielectric function $\varepsilon^*(f) = \varepsilon'(f) - i\varepsilon''(f)$ (f - frequency, ε'- real part, ε''- loss part) was measured in the frequency range from 10^{-2} Hz to 10^7 Hz by a Novocontrol high-resolution Alpha A analyzer. The dielectric measurements were carried out under isothermal conditions; a Novocontrol Quatro Cryosystem controlled the temperature with stability better than 0.1 K. The temperature was increased with steps of 5 K from 220 K to 428 K.

The model-function of Havriliak-Negami (HN-function) was employed to analyze and to separate the different relaxation processes (details in ref. [41]). The HN-function has the following form:

$$\varepsilon^*(f) - \varepsilon_\infty = \frac{\Delta\varepsilon}{(1 + (if/f_0)^\beta)^\gamma}, \tag{1}$$

where f_0 is a characteristic frequency related to the frequency of maximal loss f_p (relaxation rate) of the relaxation process under consideration, ε_∞ describes the value of the real part ε' for $f \gg f_0$. β and γ are fractional form parameters ($0 < \beta \leq 1$

and $0 < \beta\gamma \leq 1$). $\Delta\varepsilon$ denotes the dielectric strength. Conduction effects were treated in the WinDATA program by adding a conductivity contribution $\sigma_0/\varepsilon_0(2\pi f)^x$ to the dielectric loss. σ_0 is related to the *dc* conductivity of the sample and ε_0 is the dielectric permittivity of the vacuum. The parameter x ($0 < x \leq 1$) describes for $x < 1$ non-Ohmic effects in the conductivity.

The results are further discussed using the temperature dependence of the relaxation rate f_p and of the dielectric strength $\Delta\varepsilon$.

The loading degree with water c_w was estimated by thermogravimetric (TG) measurements [39]. These measurements were performed by a Diamond TG-DTA apparatus (Perkin Elmer) under dry airflow. Taking the density of confined water as $\rho_w^{conf} \approx 1\text{g/cm}^3$, the layer thickness h_w^{conf} of the confined water was roughly estimated to $h_w^{conf} = (c_w / \rho_w^{conf}) / S_{BET}$. S_{BET} is the specific surface area measured by nitrogen absorption.

3. Results and discussion

3.1. Structure of the layered oxide materials

XRD diagrams (not shown here) indicated that our materials have a layered structure; the basal spacing of (001) was estimated to be *ca.* 7.8 Å. Each layer is 0.48 nm thick [1] and contains edge-sharing octahedra. The interlayer distance is a function of the hydrating degree and of the size of the ions intercalated in the interlayer.

The interlayer voids may have prismatic or octahedral structures depending whether the opposing ions of adjacent layers like hydroxyl groups in LDH samples lie vertically above one another or offset in close packed positions.

Another important feature is the hydrogen bonding of water molecules with the surface components or with the interlayer particles. In fact, it was shown that hydrogen bonding is important for maintaining the stability of the expanded interlayer region in LDH materials [42]. Dehydration is a complex process leading to a gradual, concerted layer collapse as temperature is raised and water is lost. Compared to dehydrating, hydrating is a slow process occurring over a few days.

3.2. Thermogravimetric analysis

Representative TG curves together with their DTG derivatives are shown in Fig. 1. The thermogravimetric parameters for the LDH samples studied are summarized in Table 1.

The LDH samples undergo a progressive weight loss in four steps when the temperature increases, noted with Roman numerals. The ill-defined inflection points that can hardly be distinguished in the TG curves were better defined when comparing with the associated DTG and DTA curves. The first two weight-loss steps cover the interval till 500 K are due to the removal of weakly bonded water molecules, physisorbed on the surface or positioned in the interlayer spaces [43, 44]. At higher temperatures the chemical process of the dehydroxylation of the brucite-like layers starts, where the water molecules formed by the reaction further are desorbed. Fi-

nally a third endothermic effect, extended up to ca. 600 K, is observed. These three processes lead to the collapse of the layered structure. A fourth step or possibly even more steps has/have also chemical origins, which are related to the transformation and/or removal of the interlayer anion [43]. It is noteworthy that the dielectric measurements are performed in the low temperature range where only physical desorption processes take place and so the structure of the materials is maintained.

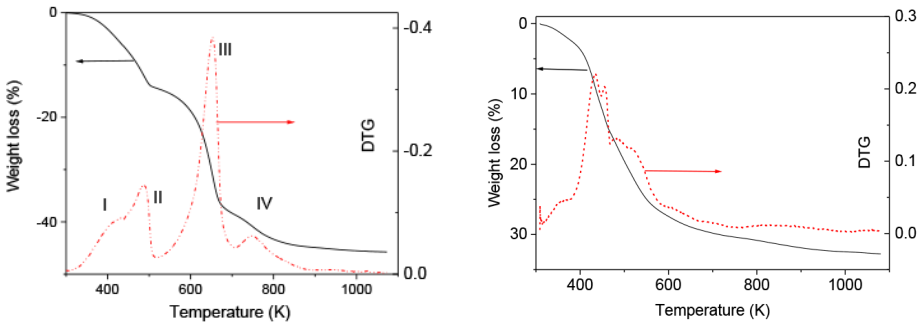

Fig. 1. TG curve (solid line) and the corresponding DTG curve (dotted line) for (a) Mg3Al-LDH; (b) Zn2Al-LDH samples.

Table 1. Water content and the estimated thickness of the water layer

Sample	Total mass loss [%]	Temp. of first step [K]	Water content# [%]	Specific surface area [m^2/g]	Equivalent water thickness [nm]	T^*_{max} [K]
Mg3Al-LDH	44.6	485	13.6	100	1.57	297
Mg3Ga-LDH	39.5	483	13.5	97	1.62	282
Zn2Al-LDH	32.7	435	14.5	96	1.76	313
Zn2Ga-LDH	23.6	453	11.8	90	1.48	282

#Water content is taken as the mass lost up to first main step.
*The equivalent water thickness was calculated considering the weight loss up to a temperature of 473 K.

More information about the structure of the layered materials related to water comes from modeling the hydration of hydrotalcites [45]. It was shown that the Al-polyhedra in the hydroxide layers are quite regular; instead, the Mg-polyhedra are distorted ones. In addition most of the Mg ions have either a water molecule or an interlayer anion coordinated thus forming a 7-coordination site. The displacement of Mg atoms from the middle of the hydroxide layers results in the formation of a much less regular network of hydrogen atoms.

The total weight loss may be used to estimate the number of interlayer water molecules. For example, the total weight loss after calcination at ca. 1073 K of sample Mg3Al-LDH amounts to ca. 44.6 % of the initial sample weight, of which dehydration accounts for 13.6 %, whereas dehydroxylation and combustion of the interlayer anion contribute around 21 %. In addition, taking into consideration the specific surface area, the thickness of the water layer was estimated.

According to Table 1, the calculated thickness of a surface layer assuming homogeneously distributed water molecules (equivalent layer thickness) is of 8-9 molecules if the dimension of a water molecule with hydrogen bonds is ∼0.2 nm. Thus one has to conclude that in the layered materials investigated, water can form clusters on the "pore" surface, which are uniformly distributed. A layer of thickness 0.4 nm of non-freezable water is found for molecular sieves [46]. It is then assumed that these clusters have a similar size because no indication for a real phase transition is found in the dielectric investigations discussed below. Nevertheless the rotational fluctuations of the water molecules in these clusters are important.

3.3. Dielectric spectroscopy

3D representative plots of the dielectric loss as function of frequency and temperature are given in Fig. 2 for Zn2Al-LDH and Zn2Ga-LDH samples.

The relaxation behavior of Mg containing samples is rather similar with that of Zn containing ones.

Several dielectric phenomena can be observed like a Maxwell-Wagner polarization effect (due to the blocking of charge carriers at the grain boundaries) and a *dc* conduction at low frequencies, as it was the case in related porous materials. The Maxwell–Wagner–Sillars peak is superimposed to the conductivity phenomenon and can be observable at low frequencies. In addition at least one dielectric relaxation process, indicated by a peak in the dielectric loss, is observed in Fig. 2. This relaxation process has to be assigned to the constrained rotational dynamics of water molecules confined in the interlayer galleries for the following reasons: It is well known that in the experimental frequency and temperature window no relaxation process due to SiO4 or to bulk liquid water molecules is expected [47, 48]. Therefore, a similar behavior is supposed for Zn2Al-LDH and Zn2Ga-LDH. Moreover, it was already shown for related AlMCM-41 [49], porous glasses [50] or Anopore membranes [51] that the contribution of the pore wall material (motions of the silica/alumina tetrahedra as building groups) to the dielectric loss is negligibly small (three orders of magnitude lower) compared to that observed for the (liquid) loaded samples. In addition, the exchanged ions generally contribute mostly to the dc conductivity [52]. Besides, after heating up the sample, no relaxation process can be observed by the dielectric measurements carried out during the cooling. This is a supplementary argument that the observed process is related to rotational fluctuations of water molecules. Consequently this process is assigned to the rotational dynamics of water molecules in the inter galleries of the LDH material.

The observed long relaxation times in comparison to bulk water leads to the conclusion that the involved water molecules are constrained and are in close contact

with the confining LDH surface. In related systems, such constrained water molecules in close contact to confining surfaces (layers) were confirmed, *e.g.* for water in MCM-41 molecular sieves, by using line shape analysis of ^{2}H double quantum filtered NMR and T_1 measurements [53].

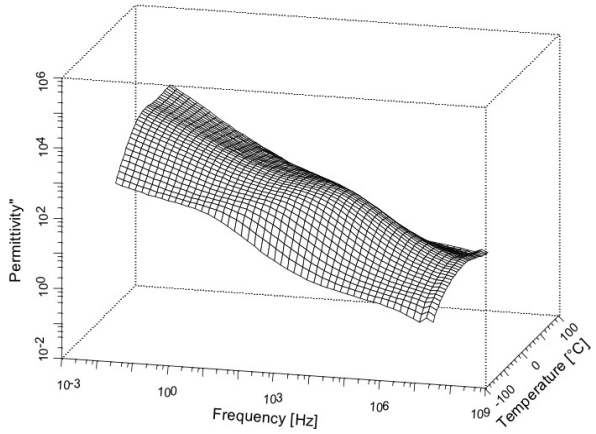

(a)

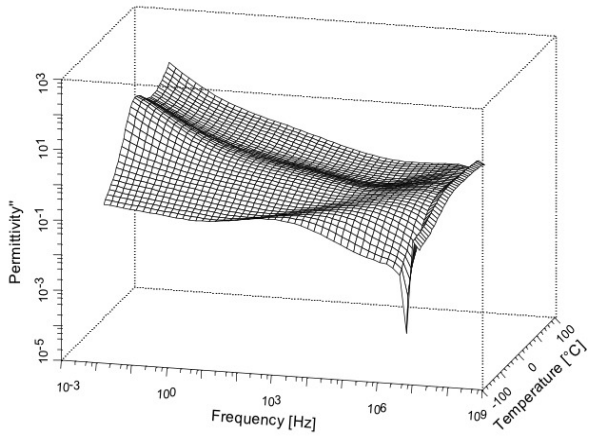

(b)

Fig. 2. Dielectric loss vs. frequency and temperature in a 3D representation for (a) Zn2Al-LDH; (b) Zn2Ga-LDHsamples.

The relaxation process has an unusual behavior with regard to the temperature dependence of its mean relaxation rate. With increasing temperature, the maximum of the dielectric loss shifts to higher frequencies, as expected. After reaching a certain temperature the maximum position of the dielectric loss moves down to lower frequencies with further increase of temperature. The temperature dependence of the relaxation rate is represented in Fig. 3.

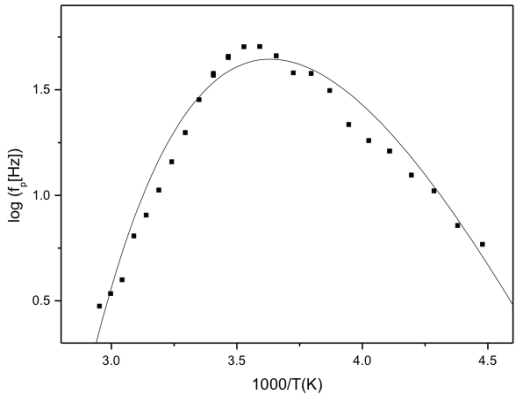

(a)

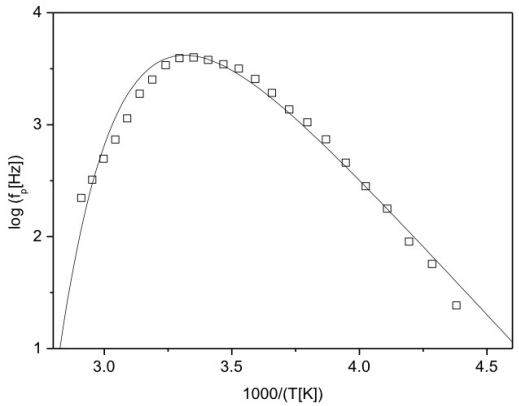

(b)

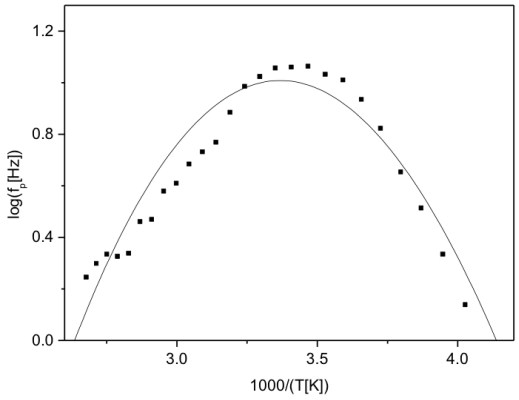

(c)

Fig. 3. Relaxation rate vs. reciprocal temperature for the samples: (a) Zn2Ga-LDH; (b) Mg3Al-LDH; (c) Mg3Ga-LDH. The line is a fit of eq. (2) to the data.

As already seen in the raw data f_p increases with temperature up a maximum value observed at T_{max}= 313 K for Zn2Al-LDH and 282 K for Zn2Ga-LDH. For temperatures higher than T_{max}, the frequency f_p decreases with further increase of temperature. This unusual temperature dependence of the relaxation rate should be not predominately related to a loss of water. First, it is noted that T_{max} is essentially lower than the temperature found for the maximal loss of water. Secondly, the dielectric strength $\Delta\varepsilon$ has a maximum with increasing the temperature in the temperature range investigated (see Fig. 4). There are changes in the temperature dependence of $\Delta\varepsilon$ around the melting point of bulk water and at T_{max}. At high temperatures a plateau level is observed. These changes might be related to different structure of the confined water. This needs further investigations.

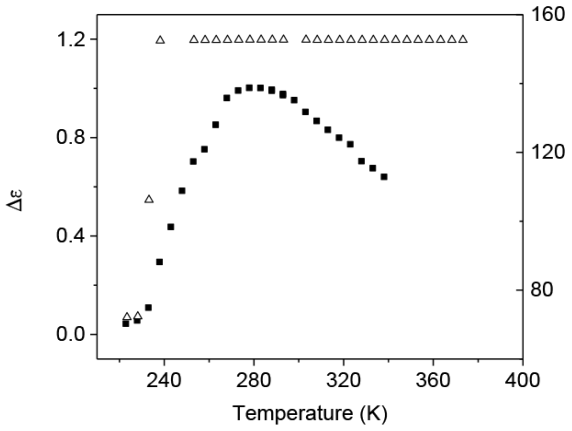

Fig. 4. Dielectric strength $\Delta\varepsilon$ *vs.* temperature for Zn2Ga-LDH (filled squares) and Mg3Ga-LDH (open up triangles) samples.

The relaxation rates of Mg containing LDH samples are also plotted versus 1/T in Fig. 3 while the variation of the dielectric strength is given in Fig. 4. Like for Zn containing LDH samples, the temperature dependence of the relaxation rates is saddle-like with a maximum temperature of T_{max} = 297 K. However, the dielectric strength has higher values than for investigated Zn containing LDHs and no maximum can be seen in the temperature dependence: Dielectric strength of Mg3Al-LDH has a small variation with the temperature (not shown here): It is only a slight change in the temperature dependence of $\Delta\varepsilon$. Based on the differences in relaxation strength and in the pattern of the relaxation times, the structure of water involved in relaxation differs, but it is still unclear how it does.

The whole temperature dependence of f_p cannot be described by an Arrhenius or Vogel/Fulcher/Tammann equations [41]; an adequate description of this unusual non-monotonous dependence can be given by the Ryabov model [37] which was also applied to describe water relaxation in the sodalite cages of faujasite and in other systems (*e.g.* [38, 39, 49]). The saddle-like temperature dependence might be due to the counterbalance of two competing processes: rotational fluctuations the molecules

obeying the Arrhenius law $\sim \exp[E_a \,/\, (k_B T)]$ (E_a is the height of the potential barrier and k_B is the Boltzmann constant); in the vicinity of a selected water molecule, a certain amount of free volume provided by a defect should be available for its reorientation. The defect concentration varies exponentially with the temperature $\sim C \exp[-E_d \,/\, (k_B T)]$ (E_d is the energy of the defect formation and C is the inverse maximum of the defect concentration). C determines mainly the value of the relaxation rate at the maximum temperature. We have:

$$\frac{1}{2\pi f_p} = \tau = \tau_\infty \exp\left[\frac{E_a}{k_B T} + C \exp\left(-\frac{E_d}{k_B T}\right)\right] \tag{2}$$

Equation 2 was fitted to the temperature dependence of the relaxation rate of our LDH samples. The estimated parameters are given in the Table 2 along with values for related systems.

Table 2. Fit parameters of the Ryabov model to the investigated LDH samples

Sample	E_a [kJ/mol]	E_d [kJ/mol]	–log (τ_∞[s])	Max. number of defects	References
Mg3Al-LDH	47.2	33.8	12.4	6.0×10^{17}	This work
Mg2Ga-LDH	64.0	12.3	14	8.3×10^{20}	This work
Zn2Al-LDH	73.2	18.4	17.9	1×10^{20}	[28], This work
Zn2Ga-LDH	47.6	13.0	12.2	5.4×10^{19}	[28], This work
NiAlMo$^{\#}$	97.7	14.2	20.6	10^{20}	[39]
ZnAlMo$^{\#}$	75.4	10.5	17.3	1.5×10^{20}	[39]
AlSBA-15	50.8	25.4	13.0	10^{19}	[38]
NMSF	48.1	31.3	12.8	10^{18}	[38]
Porous glass	55-42	39-30	13.5-12.1	$10^{16} - 10^{17}$	[37]

$^{\#}$ LDH structure, molybdate ions in the interlayer.

The maximum number of defects per mole of adsorbed water is estimated in the range from 10^{20} to 10^{21} for these LDH materials. These values are a bit higher than those found for water confined to nanoporous materials such as glasses, AlSBA-15 or nanoporous molecular sieves with foam-like structure. They are even higher compared to that found in bulk ice (cited in ref. [39]). This might suggest that more defects can be formed in water adsorbed in the layered oxide materials than in nanoporous molecular sieves/glasses or in bulk ice. So in the layered oxide materials there are more possibilities for defect formation than in the other confining systems. Spectroscopic investigations have indeed shown the presence of some extra material in the interlayer voids which might play the role of the defects [40] but this fact must be supported by other studies as well.

There is a correlation between the value of the energy of defect formation E_d and the number of defects of the absorbed water structure: thus, for samples with a lower

E_d value the number of defects is higher. This seems to be reasonable, because the lower is the energy of defect formation, the more defects can be formed.

The values found for the activation energy in the LDH materials are comparable with those found for related materials (see Table 2). This might be due to confinement effects of the inter galleries on the structure of embedded water which changes the internal rotational barriers. It can be observed that –log τ_∞ increases with the activation energy E_a.

The values of the activation energy E_a (Table 2) are smaller than those found for proton hopping between neighboring Al-sites in molecular sieves (89–126 kJ mol^{-1}) [42]. So these values might argue against a proton hopping mechanism. Moreover the number of protons is very small in the case of present LDH-type materials and therefore proton contribution to the dielectric loss is less probable.

The samples used for the dielectric measurements consist of pressed pellets. Then the absolute values of the dielectric strength cannot be compared directly. It has been then proposed [39] to compare the dielectric strength of the samples when normalized to the value corresponding to the lowest (measured) temperature. However, it become obvious from Figs. of above that no clear effect can be seen in such relative representations, except Zn2Ga-LDH sample for which, the curvature of the temperature dependence increases more than in the simple representation. The observed behavior of the dielectric strength cannot be explained by considering the thickness of the water layer as well, since the latter has similar values for all the investigated samples. The interlayer distance is also comparable in all the investigated samples. More experiments are thus necessary to elucidate this behavior.

A final point to be noted regards the real part σ' of the complex conductivity of the samples, which seems to be rather high especially in the case of Al and Mg containing samples, while Zn2Ga-LDH has the lowest conductivity among these samples (see Fig. 5). Conductivity depends on the temperature (concentration of charge carriers) [41]b] and their mobility. Our samples behave as ionic conducting disordered materials, which did not have the clear plateau on the low frequency side, due to a still low temperature. Supposing the carrier mobility comparable for the studied samples, it would result that the Zn2Ga-LDH sample has the smallest number of such carriers and Mg3Al-LDH, the highest number. In fact, the high concentration of counter ions is responsible for the high electrode polarisation effects, which are particularly visible on the low-frequency side.

As it was already mentioned [39], one key parameter to model the temperature dependence of the relaxation times in the Ryabov model is the existence of defects. However, as it was discussed as well in ref. [39], the question of the nature of the defects in these and related systems is still open. In the case of the layered oxide materials, the H bonds might involve in addition the oxygen atoms of interlayer water or of the charge compensating ions. The interlayer composition and in turn the composition of the sheets has then to play an important role as well.

The fit parameters can be thus used to evaluate the effects appeared in the studied samples due to the additional OH groups or ions.

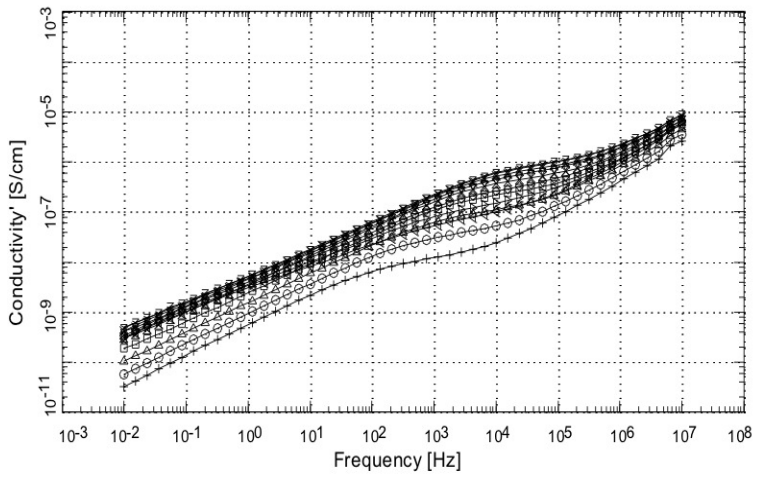

(a)

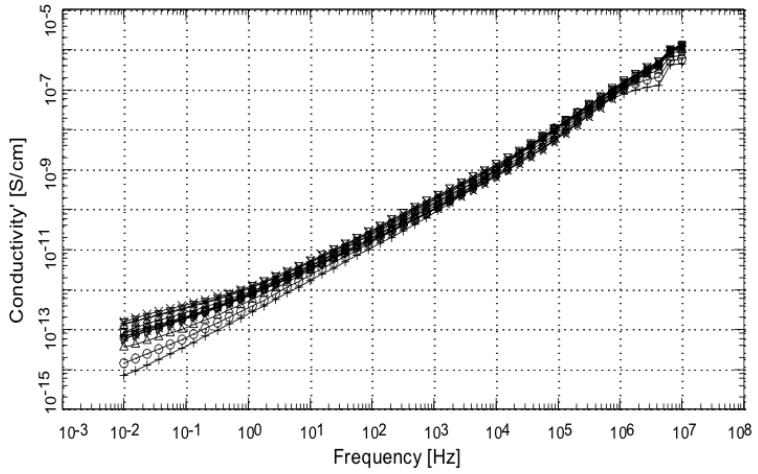

(b)

Fig. 5. Real part of the conductivity σ' as function of the frequency for the samples: (a) Mg3Al-LDH; (b) Zn2Ga-LDH. The temperature increases with the same steps from bottom to top between 233 and 343 K, in both representations.

4. Conclusions

Layered double hydroxides containing Al or Ga as the trivalent ions and Mg or Zn as bivalent ions were investigated by broadband dielectric spectroscopy in a wide temperature range. Besides conduction effects at least a relaxation process was observed which is assigned to the reorientational fluctuations of water molecules adsorbed on

the oxide surface or in the interlayer voids. A non-monotonous temperature dependence of the relaxation rates of this relaxation process has been found. A quantitative description of this dependence was possible based on a model assuming two competing processes: rotational fluctuation of water molecules and formation of additional defects. Reasonable values for the characteristic parameters were obtained.

It is found that the behavior water in the studied layered oxide with brucite structure is similar to that observed for water in porous glasses and molecular sieves. But the activation energy of the rotational fluctuation, the pre exponential factor and the number of defects are higher whereas the value of the energy of defect formation is lower in the layered oxide materials than for water confined to nanoporous molecular sieves, porous glasses or in bulk ice.

Hydrogen bonds formed in the water might involve the oxygen atoms of the surface hydroxyl groups or of the charge compensating ions.

The interlayer composition has then to play an important role in the rotational dynamics of water as well.

The characteristic parameters resulted from the applied model can be used to evaluate the effects appeared due to surface hydroxyl groups or interlayer ions.

The rather high dielectric response of LDH materials is due to the two charge carriers, the water protons and the inter gallery ions.

Acknowledgments. The financial support of Romanian Authority UEFISCDI by CORE Program (for LF, SF, CPG and IZ) and by 29/2012 Project (for FN and VIP) is gratefully acknowledged.

References

[1] CAVANI F., TRIFIRÒ F., VACCARI A., *Hydrotalcite-type anionic clays: preparation, properties and applications*, Catal. Today, Vol. **11**, No. 2, 1991, pp. 173–301.

[2] XU Z.P., ZHANG J., ADEBAJO M.O., ZHANG H., ZHOU C., *Catalytic applications of layered double hydroxides and derivatives*, Appl. Clay Sci., Vol. **53**, No. 2, 2011, pp. 139–150.

[3] ZÜMREOGLU-KARAN B., AY A., *Layered double hydroxides - multifunctional nanomaterials*, Chem. Papers., Vol. **66**, No. 1, 2012, pp. 1–10.

[4] AHMED N., SHIBATA Y., TANIGUCHI T., IZUMI Y., *Photocatalytic conversion of carbon dioxide into methanol using zinc–copper–M(III) (M = aluminum, gallium) layered double hydroxides*, J. Catal., Vol. **279**, No. 1, 2011, pp. 123–135.

[5] KAWAMURA S., AHMED N., CARJA G., IZUMI Y., *Photocatalytic Conversion of Carbon Dioxide Using Zn–Cu–Ga Layered Double Hydroxides Assembled with Cu Phthalocyanine: Cu in Contact with Gaseous Reactant is Needed for Methanol Generation*, Oil & Gas Sci. Technol., Vol. **70**, No. 5, 2015, pp. 841-852.

[6] HIRATA N., TADANAGA K., TATSUMISAGO M., *Photocatalytic O2 evolution from water over Zn–Cr layered double hydroxides intercalated with inorganic anions*, Mater. Res. Bull., Vol. **62**, 2015, pp.1–4.

[7] ABELLAN G., MARTI-GASTALDO C., RIBERA A., CORONADO E., *Hybrid Materials Based on Magnetic Layered Double Hydroxides: A Molecular Perspective*, Acc. Chem. Res., Vol. **48**, No. 6, 2015, pp. 1601–1611.

[8] SALIH E.Y., ABBAS Z., AL ALI S.H.H., HUSSEIN M.Z., *Dielectric Behaviour of Zn/Al-NO3 LDHs Filled with Polyvinyl Chloride Composite at Low Microwave Frequencies*, Adv. Mater. Sci. Engn., Article No. 647120, 2014, 6p.

[9] YU W., DU M., YE W., LV W., ZHENG Q., *Relaxation behavior of layered double hydroxides filled dangling chain-based polyurethane/polymethyl methacrylate nanocomposites*, Polymer, Vol. **55**, No. 10, 2014, pp. 2455–2463.

[10] DONG Y., LIU Y., YIN J., ZHAO X., *Preparation and enhanced electro-responsive characteristic of graphene/layered double-hydroxide composite dielectric nanoplates*, J. Mater. Chem. C, Vol. **2**, No. 48, 2014, pp. 10386–10394.

[11] SHAN D., COSNIER S., MOUSTY C., *Layered Double Hydroxides: An Attractive Material for Electrochemical Biosensor Design*, Anal. Chem., Vol. **75**, No. 15, 2003, pp. 3872–3879.

[12] JAYALAKSHMI M., BALASUBRAMANIAN K., *Simple Capacitors to Supercapacitors – An Overview*, Int. J. Electrochem. Sci., Vol. **3**, No. **11**, 2008, pp. 1196–1217.

[13] GE X., GU C., YIN Z., WANG X., TU J., LI J., *Periodic stacking of 2D charged sheets: Self-assembled superlattice of Ni-Al layered double hydroxide (LDH) and reduced graphene oxide*, Nanoenergy, Vol. **20**, 2016, pp. 185–193.

[14] GUAN S., LIANG R., LI C., YAN D., WEI M., EVANS D.G., DUAN X., *A layered drug nanovehicle toward targeted cancer imaging and therapy*, J. Mater. Chem. B, Vol. **4**, No. 7, 2016, pp. 1331–1336.

[15] WANG S., GAO B., LI Y., ZIMMERMAN A.R., CAO X., *Sorption of arsenic onto Ni/Fe layered double hydroxide (LDH)-biochar composites*, RSC Adv., Vol. **6**, No. 22, 2016, pp. 17792–17799.

[16] EHSAN K.N., XIN W., DE-YI W., *Multifunctional intercalation in layered double hydroxide: toward multifunctional nanohybrids for epoxy resin*, J. Mater. Chem. A, Vol. **4**, No. 6, 2016, pp. 2147–2157.

[17] FORUZIN L.J., REZVANI Z., NEJATI K., *Fabrication of TiO2@ZnAl-layered double hydroxide based anode material for dye-sensitized solar cell*, RSC Adv., Vol. **6**, No. 13, 2016, pp. 10912–10918.

[18] SCHÖNHALS A., GOERING H., COSTA F.R., WAGENKNECHT U., HEINRICH G., *Dielectric properties of nanocomposites based on polyethylene and layered double hydroxide*, Macromolecules, Vol. **42**, No. 12, 2009, pp. 4165–4174.

[19] PUROHIT P.J., HUACUJA-SÁNCHEZ J.E., WANG D.Y., EMMERLING F., THÜNEMANN A., HEINRICH G., SCHÖNHALS A., *Structure–property relationships of nanocomposites based on polypropylene and layered double hydroxides*, Macromolecules, Vol. **44**, No. 11, 2011, pp. 4342–4354.

[20] PUROHIT P.J., WANG D.Y., EMMERLING F., THÜNEMANN A.F., HEINRICH G., SCHÖNHALS A., *Arrangement of layered double hydroxide in a polyethylene matrix studied by a combination of complementary methods*, Polymer, Vol. **53**, No. 11, 2012, pp. 2245–2254.

[21] AHMED A.A.A., TALIB Z.A., BIN HUSSEIN M.Z., ZAKARIA A., *In situ dielectric measurements of Zn-Al layered double hydroxide with anionic nitrate ions*, Solid State Sci., Vol. **14**, No. 8, 2012, pp. 1196–1202.

[22] ELMELOUKY A., EL MOZNINE R., LAHKALE R., SADIK R., SABBAR EL., CHAHID EL., CHOUKRI EL., MEZZANE D., BELBOUKHARI A., *Analysis of conduction mechanism in lamellar double hydroxide by impedance spectroscopy*, J. Optoelectron. Adv. Mater. Vol. **15**, No. 11, 2013, pp. 1239–1247.

[23] BUGRIS V., HASPEL H., KUKOVECZ Á., KÓNYA Z., SIPICZKI M., SIPOS P., PÁLINKÓ I., *Rehydration of dehydrated CaFe-L(ayered)D(ouble)H(ydroxide) followed by thermogravimetry, X-ray diffractometry and dielectric relaxation spectroscopy*, J. Molec. Struct., Vol. **1044**, 2013, pp. 26–31.

[24] PUROHIT P.J., WANG DE-YI, WURM A., SCHICK C., SCHÖNHALS A., *Comparison of thermal and dielectric spectroscopy for nanocomposites based on polypropylene and Layered Double Hydroxide - Proof of interfaces*, Eur. Polymer J., Vol. **55**, 2014, pp. 48–56.

[25] ELMELOUKY A., MORTADI A., EL MOZNINE R., CHAHID EL., LAHKALE R., *Analysis of Conduction Mechanism in Zn_2FeNO_3 using Impedance Spectroscopy*, Intern. J. Adv. Res. Phys. Sci., Vol. **2**, No. 11, 2015, pp. 1–10.

[26] AHMED A.A.A., TALIB Z.A., HUSSEIN M.Z., *Influence of sodium dodecyl sulfate concentration on the photocatalytic activity and dielectric properties of intercalated sodium dodecyl sulfate into Zn-Cd-Al layered double hydroxide*, Mater. Res. Bull., Vol. **62**, 2015, pp. 122–131.

[27] LENG J., PUROHIT P.J., KANG N., WANG DE-YI, FALKENHAGEN J., EMMERLING F., THÜNEMANN A.F., SCHÖNHALS A., *Structure-property relationships of nanocornposites based on polylactide and MgAl layered double hydroxide*, Eur. Polymer J., Vol. **68**, 2015, pp. 338–354.

[28] FRUNZA L., GANEA C.P., ZGURA I., FRUNZA S., NEATU F., PARVULESCU V.I., *Layered materials of LDH-type containing Zn ions Dielectric measurements show rotational fluctuations of water molecules*, Semiconductor Conference (CAS), 2015 International, 12-14 Oct. 2015, Sinaia, pp. 67–70, DOI 10.1109/SMICND.2015.7355162.

[29] CARRIAZO D., MARTÝN C., RIVES V., POPESCU A., COJOCARU B., MANDACHE I., PARVULESCU V.I., *Hydrotalcites composition as catalysts: Preparation and their behavior on epoxidation of two bicycloalkenes,* Micropor, Mesopor. Mater., Vol. **95**, No. 1-3, 2006, pp. 39–47.

[30] NEATU F., CIOBANU M., STOFLEA L., FRUNZA L., PARVULESCU V., MICHELET V., *Arylation of alkynes over hydrotalcite docked Rh-m-TPPTC complex*, Catal. Today, Vol. **247**, No. 1, 2015, pp. 155–162.

[31] BIDADI H., SCHROEDER P.A., PINNAVAIA T.J., *Dielectric properties of montmorillonite clay films: Effects of water and layer charge reduction*, J. Phys. Chem. Solids, Vol. **49**, No. 12, 1988, pp. 1435–1440.

[32] HELMY A.K., SANTAMARIA R.M., GARCIA N.J., *Dielectric behaviour of dry montmorillonite discs*, Colloids Surf., Vol. **34**, No. 1, 1988–1989, a) pp. 13-21; b) pp. 345–352.

[33] HELMY A.K., SANTAMARIA R.M., GARCIA N.J., *Dielectric behaviour of montmorillonite quinoline complexes*, Colloids Surf. Vol., **40**, 1989, pp. 227–233.

[34] DUDLEY L.M., BIALKOWSKI S., OR D., JUNKERMEIER C., *Low Frequency Impedance Behavior of Montmorillonite Suspensions: Polarization Mechanisms in the Low Frequency Domain*, Soil Sci. Soc. Am. J., Vol. **67**, No. 2, 2003, pp. 518–526.

[35] JACOBS J. D., KOERNER H., HEINZ H., FARMER B.L., MIRAU P., GARRETT P.H., VAIA R.A., *Dynamics of Alkyl Ammonium Intercalants within Organically Modified Montmorillonite: Dielectric Relaxation and Ionic Conductivity*, J. Phys. Chem. B, Vol. **110**, No. 41, 2006, pp. 20143–20157.

[36] VASILYEVA M. A., GUSEV YU A., SHTYRLIN V.G., *Two types of adsorbed water in natural montmorillonites at low temperatures by dielectric spectroscopy*, J. Phys.: Conf. Ser. Vol. **394**, 2012, 012027.

[37] RYABOV YA., GUTINA A., ARKHIPOV V., FELDMAN YU., *Dielectric Relaxation of Water Absorbed in Porous Glass*, J. Phys. Chem. B, Vol. **105**, No. 9, 2001, pp. 1845–1850.

[38] FRUNZA L., KOSSLICK H., PITSCH I., FRUNZA S., SCHÖNHALS A., *Rotational Fluctuations of Water inside the Nanopores of SBA-Type Molecular Sieves*, J. Phys. Chem. B, Vol. **109**, No. 18, 2005, pp. 9154–9159.

[39] FRUNZA L., SCHÖNHALS A., FRUNZA S., PARVULESCU V.I., COJOCARU B., CARRIAZO D., MARTÍN C., RIVES V., *Rotational fluctuations of water confined to layered oxide materials: nonmonotonous temperature dependence of relaxation times*, J. Phys. Chem. A, Vol. **111**, No. 24, 2007, pp. 5166–5175.

[40] FRUNZA L., GHEORGHE N., IOVA F., GANEA P., NEATU F., PARVULESCU V.I., *Spectroscopic Analysis of the Interstitial Anions in Some Layered Double Hydroxide Materials*, Rev. Chimie (Bucuresti) Vol. **62**, No.8, 2011, pp. 766–772.

[41] KREMER F., SCHÖNHALS A., *Broadband Dielectric Spectroscopy*, Springer-Verlag, Berlin Heidelberg, 2003, a) pp. 99–129; b) pp. 475ff.

[42] VUCELIC M., MOGGRIDGE G. D., JONES W., *Thermal Properties of Terephthalate- and Benzoate-Intercalated LDH*, J. Phys. Chem., Vol. **99**, No. 20, 1995, pp. 8328–8337.

[43] RIVES V., *Characterisation of layered double hydroxides and their decomposition products,* Mater. Chem. Phys., Vol. **75**, No. 1-3, 2002, pp. 19–25.

[44] JAUBERTIE C., HOLGADO M. J., SAN ROMAN M. S., RIVES V., *Structural Characterization and Delamination of Lactate-Intercalated Zn,Al-Layered Double Hydroxides*, Chem. Mater. Vol. **18**, No. 13, 2006, pp. 3114–3121.

[45] KALINICHEV A., KIRKPATRICK R. J., CYGAN R. T., *Molecular modeling of the structure and dynamics of the interlayer and surface species of mixed-metal layered hydroxides: Chloride and water in hydrocalumite (Friedel's salt)*, Am. Mineral., Vol. **85**, No. 7-8, 2000, pp. 1046–1052.

[46] MORISHIGE K., IWASAKI H., *X-ray Study of Freezing and Melting of Water Confined within SBA-15*, Langmuir, Vol. **19**, No. 7, 2003, pp. 2808–2811.

[47] HENCH L. L., WEST J. K., *The sol-gel process*, Chem. Rev. Vol. **90**, No. 1, 1990, pp. 33–72 and references herein.

[48] DA SILVA A., DONOSO P., AERGERTER M. A., *Properties of water adsorbed in porous silica aerogels*, J. Non-cryst. Solids, Vol. **145**, 1992, pp. 168–174.

[49] FRUNZA S., FRUNZA L., SCHONHALS A., ZUBOWA H-L, KOSSLICK H., CARIUS H.-E.,. FRICKE R, *On the confinement of liquid crystals in molecular sieves: dielectric measurements*, Chem. Phys. Lett., Vol. **307**, No. 1–3, 1999, pp. 167–176.

[50] ALIEV F. M., NAZARIO Z., SINHA G., *Broadband dielectric spectroscopy of confined liquid crystals*, J. Non-Cryst. Solids, Vol. **305**, 2002, pp. 218–225.

[51] ROZANSKI R., STANNARIUS H., GROOTHUES F., KREMER F., *Dielectric properties of the nematic liquid crystal 4-n-pentyl-4'-cyanobiphenyl in porous membranes*, Liq. Cryst., Vol. **20**, No. 1, 1996, pp. 59–66.

[52] FRANKE M.E., SIMON U., *Proton mobility in H-ZSM5 studied by impedance spectroscopy*, Solid State Ionics, Vol. **118**, No. 3-4, 1999, pp. 311–316.

[53] HWANG D. W., SINHA A.K., CHENG C.Y., YU T.Y., HWANG L. P., *Water Dynamics on the Surface of MCM-41 via 2H Double Quantum Filtered NMR and Relaxation Measurements*, J. Phys. Chem. B, Vol. **105**, No. 24, 2001, pp. 5713–5721.